Sains Malaysiana 54(6)(2025): 1583-1592
http://doi.org/10.17576/jsm-2025-5406-13

Improved Performance of P3HT:PCBM-Based Inverted Organic Solar Cell using SnO_2/ZnO Electron Transport Bilayer for Low Light Application

(Peningkatan Prestasi Sel Suria Organik Songsang Berasaskan P3HT: PCBM menggunakan Dwilapisan Pengangkutan Elektron SnO_2/ZnO untuk Aplikasi Cahaya Rendah)

NOORAKMAR HIDAYAH BINTI MOHAMED HASHINI[1,2], MOHAMMAD HAFIZUDDIN HJ JUMALI[1] & CHI CHIN YAP[1,*]

[1]*Department of Applied Physics, Faculty of Science and Technology, Universiti Kebangsaan Malaysia, 43600 UKM Bangi, Selangor, Malaysia*
[2]*Centre of Foundation Studies, Universiti Teknologi MARA, Cawangan Selangor, Kampus Dengkil, 43800 Dengkil, Selangor, Malaysia*

Received: 23 December 2024/Accepted: 4 April 2025

ABSTRACT

Organic solar cells (OSCs) have attracted much research attention due to their advantages such as low cost, easy processing, light weight, flexible and suitable for large-scale production. ZnO has shown to be an effective electron transport layer (ETL) in OSCs. However, it also suffers from various defects on its surface and improperly matched work function with the photoactive layer which then hinders electron extraction and conduction in OSCs. Hence, in this work, due to its favorable attributes such as high electron mobility, wide bandgap as well as deep conduction and valence band, SnO_2 was chosen in this study as cathode interfacial layer placed in stacked structure with ZnO. This study intends to improve the power conversion efficiency (PCE) of poly(3-hexylthiophene-2,5-diyl) (P3HT): (6,6)-phenyl-C61-butyric-acid-methyl-ester (PCBM) based inverted OSCs by exploiting the properties of SnO_2 and ZnO as bilayer ETL. The ETL was inserted between transparent fluorine-doped tin oxide (FTO) and P3HT:PCBM photoactive layer. Experimental analysis of the different configurations of ETL (ZnO only, SnO_2/ZnO, and ZnO/SnO_2) toward the PCE of inverted type OSCs was presented. The SnO_2 layer was synthesized via sol-gel spin coating method. Under both 1-Sun and white LED illumination, the devices with SnO_2/ZnO ETL demonstrated the highest PCE of 1.01% and 1.62%, respectively, with 63% and 30% enhancement compared to the control device with ZnO only ETL. Our results suggest that by depositing the SnO_2 layer before the ZnO layer, it can enhance the optical transmission, decrease the surface roughness and provide a well-matched energy level.

Keywords: Electron conduction; indoor; optical transmission; organic photovoltaic; work function

ABSTRAK

Sel suria organik (OSC) dilihat semakin menarik perhatian dalam bidang penyelidikan disebabkan oleh kelebihannya seperti ringan, fleksibel, memerlukan fabrikasi yang mudah serta murah dan amat sesuai dalam penyediaan berskala besar. Kajian terdahulu membuktikan bahawa ZnO adalah bahan yang baik dan berkesan sebagai lapisan pengangkut elekton (ETL) dalam OSC. Namun begitu, masih terdapat banyak kelemahan pada lapisan ZnO yang perlu diatasi seperti kecacatan pada permukaan serta fungsi tenaga yang tidak sesuai dengan lapisan fotoaktif yang membantutkan pengekstrakan dan pemindahan elektron di dalam OSC. Dalam kajian ini, SnO_2 telah dipilih untuk digunakan sebagai lapisan tambahan untuk membentuk ETL dwilapisan disebabkan kadar konduktiviti elektronnya yang tinggi, jurang tenaga yang besar serta jalur valensi dan konduksi yang lebih dalam. Kajian ini bertujuan untuk meningkatkan kecekapan penukaran kuasa (PCE) peranti OSC songsang berasaskan poli (3-heksilthiofena-2,5-dil) (P3HT):(6,6)-fenil-C_{61} asid butrik metal ester (PCBM) dengan menggabungkan kelebihan ZnO dan SnO_2. ETL dimendapkan di antara lapisan oksida timah terdop fluorin (FTO) dan lapisan fotoaktif P3HT:PCBM. Penyelidikan uji kaji untuk konfigurasi ETL yang berbeza (ZnO, SnO_2/ZnO dan ZnO/SnO_2) terhadap PCE OSC songsang dibentangkan. Lapisan SnO_2 disediakan dengan menggunakan kaedah sol-gel dan salutan putaran. Hasil keputusan menunjukkan peranti dengan ETL SnO_2/ZnO menghasilkan PCE tertinggi di bawah kedua-dua keadaan pencahayaan 1-matahari (1.01%) serta pencahayaan LED putih (1.62%). Keputusan ini mencatatkan peningkatan prestasi masing-masing sebanyak 63% dan 30% berbanding peranti kawalan dengan ETL lapisan tunggal ZnO. Hasil kajian ini menunjukkan apabila lapisan SnO_2 dimendapkan sebelum lapisan ZnO, ia membantu meningkatkan penghantaran optik, mengurangkan kekasaran permukaan dan menyediakan aras tenaga yang berpadanan.

Kata kunci: Dalam bangunan; fotovoltaik organik; fungsi tenaga; pemindahan elektron; penghantaran optik

INTRODUCTION

Although organic solar cells (OSCs) are still struggling to achieve high power conversion efficiency (PCE) compared to inorganic photovoltaics, much research carried out has shown that OSCs are reliable and have a remarkable potential as an effective indoor energy harvester. In doing so, due to the substantially different indoor and outdoor light conditions, particularly their intensities and irradiance spectra, modifications need to be carried out. Under indoor light conditions, number of incident photons is drastically reduced. Hence, in making modifications, it is crucial to ensure light absorption is maximized and leakage current is minimized in order to produce efficient indoor OSCs (Mohamed Nafeer Wajidh et al. 2024). In modifying the indoor OSCs, it is crucial for the electron transport layers (ETLs) to possess a sufficiently low work function to avoid surface recombination and minimize potential loss. The interfaces between the inorganic ETL and organic photoactive layer are also crucial in providing stability and efficiency, thereby contributing to an improvement in the overall indoor performance for the OSCs (Shim et al. 2012; Zhou et al. 2012). Metal oxides have shown to be an efficient electrode modifier to improve open-circuit voltage (V_{oc}), short circuit current density (J_{sc}), and fill factor (FF).

Numerous n-type metal oxides have been explored as ETLs in inverted OSCs such as SnO_2 (Suo et al. 2023), ZnO (Tarique et al. 2024), WO_3 (Mahajan et al. 2022), In_2O_3 (Omarbekova et al. 2022), TiO_2 (Wang & Tan 2022) and Bi_2S_3 (Nurul Nadhirah & Chi Chin 2022). Among them, TiO_2 and ZnO are the most used ETLs as they have been shown to produce high efficiency OSCs. However, these low work function metal oxides suffer from photocatalytic effects (Günther et al. 2023; Jiang et al. 2019; Nam et al. 2018), which contributes to decomposition of organic photoactive materials. They also have relatively low charge carrier mobility (Mussabekova et al. 2023). Besides that, ZnO experiences photoinduced shunts that increase carrier recombination losses when exposed to ultraviolet light (Yang et al. 2020), and thus negatively affecting device lifetime (Gao et al. 2022; Yao et al. 2020; Yu et al. 2022b). Besides that, sol–gel processed ZnO ETL also possess surface and inside defects such as oxygen vacancies and free surface hydroxyl group which act as recombination centers of the photogenerated charge and sensitive to oxygen and moisture in air (Yang & Yu 2023). These defects and improperly matched work function in ZnO ETL also hinders the ability of charge transport in OSCs, resulting in poor photovoltaic performance.

Among the ways identified to resolve problems with inorganic metal oxide ETLs in inverted OSCs is through interfacial modification and surface treatment. A recent study (Li, Yu & Yu 2024) had shown that when ZnO ETL was modified with 2D $ZrSe_2$, the PCEs of PBDB-T:ITIC, PM6:Y6 and PM6:L8-BO based devices have been improved by enhancing the conductivity of ZnO. The oxygen vacancy density on the ZnO surface has been reduced through interfacial modification. In addition, when ZnO nanoparticles were integrated with a ZnO layer to produce a bilayer ETL in PTB7-Th:IEICO-4F and PM6:Y6 based devices, the ability of ZnO films to extract and carry charges has been enhanced due to the formation of a better crystallinity and smoother film surface compared to single layer ZnO ETL. This had contributed to a better interfacial connection between the photoactive layer and the ETL which then improved the PCE of the devices (Tarique et al. 2024).

In this work, an in-depth study was carried out on ETLs comprising of a combination of SnO_2 and ZnO ETLs. The bilayer ETL was employed to combine the advantage of both ZnO and SnO_2. The ZnO serves as the efficient ETL with its low toxicity, high conductivity and good electron extraction capability while the SnO_2 layer can reduce the surface defects of FTO and block holes effectively, leading to an elevated electron collection and suppressed carrier recombination at the interface. In comparison to the control device with ZnO only ETL, the devices with SnO_2/ZnO ETL showcased a PCE increment of 63% and 30%, respectively, under both 1-Sun and white LED illumination.

MATERIALS AND METHODS

The fluorine-doped tin oxide (FTO) glasses with a sheet resistance of 8 Ω/sq were provided by Greatcell Solar, while the zinc acetate dihydrate (≥ 99.0%) and diethanolamine (DEA; ≥ 99.0%) were provided by Sigma Aldrich. Regioregular poly(3-hexylthiophene-2,5-diyl), commonly known as P3HT was purchased from Rieke Metals and (6,6)-phenyl-C61-butyric-acid-methyl-ester (PCBM) that served as the electron acceptor was purchased from Lumtec (≥99.5%). The precursor tin(II) chloride dihydrate ($SnCl_2.2H_2O$) was purchased from Sigma Aldrich. All materials were used directly without further purification.

In this study, inverted type OSCs were prepared. The samples were built on 1.5 × 2.0 cm glasses pre-coated with FTO. The FTO substrates were cleaned successively with deionised water, acetone and isopropanol, each for 15 min and dried (Sabri et al. 2017). The ZnO sol-gel was prepared from a mixture of 0.2 M zinc acetate dehydrate and 0.2 M DEA in absolute ethanol. The solution was stirred at 60 °C for 30 min and left to age. The SnO_2 solution was prepared by dissolving 0.2 M $SnCl_2.2H_2O$ in ethanol. The precursor solution was then stirred at 400 rpm at 80 °C for 2 h. The devices were prepared with different configurations of ETL. In the case of SnO_2/ZnO ETL, the SnO_2 layer was first deposited via spin coating at 3000 rpm for 30 s on the FTO substrate. The samples were then pre-annealed for 5 min before going through annealing in the furnace at 300 °C for 1 h. The ZnO layer was then deposited on top of the SnO_2 layer at 3000 rpm for 30 s. The spin coating process was repeated three times before the samples were annealed in the furnace at 300 °C for 1 h to form a dense

ZnO layer. For ZnO/SnO_2 ETL samples, the same method of deposition was used to deposit three layers of ZnO on the FTO substrate. The samples were then annealed at 300 °C for 1 h. When the samples have reached room temperature, the SnO_2 layer was then deposited on top of the ZnO layer via spin coating. The samples were pre-annealed for 5 min before being put into the furnace and annealed at 300 °C for 1 h. For the preparation of the photoactive layer, the PCBM and P3HT with a weight ratio of 1: 1.5 were added to the chlorobenzene solvent at a total concentration of 25 mg/mL and then stirred at 60 °C at 850 rpm overnight. The photoactive layer was then deposited at 900 rpm for 1 min on the ETL and the samples were annealed at 130 °C for 30 min. After the deposition of the photoactive layer, the Ag electrode was deposited by thermal evaporation in a vacuum of 5×10^{-5} mbar. The active area of the samples was 0.07 cm^2. For comparison, a control device with ZnO only ETL was also fabricated. The device configuration is presented in Figure 1.

The ETL thin films characteristics were investigated by a series of measurements. The morphology and cross-sectional images of the samples were observed using a Zeiss Merlin Compact field emission scanning electron microscope (FESEM) at an accelerating voltage of 3 kV. The transmission spectra of the samples were analysed using a PerkinElmer Lambda 900 UV–Vis–NIR spectrophotometer in the wavelength range of 300 – 800 nm. Steady-state photoluminescence (PL) characteristics of the photoactive layer deposited on top of various ETLs in the wavelength range of 550 to 800 nm were obtained using an Edinburg FLS920 fluorescence spectrometer at an excitation wavelength of 515 nm. Park NX-10 atomic force microscope (AFM) was used to determine the roughness and work function of ETLs. The current density-voltage (J-V) measurements of the devices were measured using a Keithley 2401 source measurement unit under the illumination of a Newport 66902 AM1.5G solar simulator at 100 mW cm^{-2} and a white LED light at 1000 lx. The parameters obtained from this measurement were V_{oc}, J_{sc}, FF and PCE.

RESULTS AND DISCUSSION

Figure 2(a)-2(d) shows the cross-sectional while Figure 2(e)-2(h) shows the top surface images of the various ETL obtained from FESEM. Figure 2(a) and 2(e) shows the surface of the sample after a layer of SnO_2 was deposited and annealed on the FTO. The packed FTO underneath could still be clearly seen, indicating the SnO_2 layer was not properly formed. Due to the low coverage of the SnO_2, the layer was unable to cover the surface of FTO thoroughly and hence the rough and irregular-sized particles on the FTO surface could still be seen. However, when the ZnO (Figure 2(b) and 2(f)) was deposited and annealed on the FTO, the stony and rough structure of the FTO started to reduce and the particles started to expand and spread out better. The FTO at the bottom was also no longer visible. When the samples were prepared with bilayer where the SnO_2 layer was placed in between the FTO and ZnO layer (Figure 2(c) and 2(g)), the thin film became smoother and the ZnO particles were more regular. The improvement of the surface could be due to the filling of SnO_2 particles in the space in between the FTO particles. With the addition of the ZnO layer above the SnO_2 layer, the thickness of the thin film increased and some of the interfacial defects could be filled. With a more uniform and smoother FTO surface, it provides a better platform to produce a better foundation and better quality ZnO and photoactive layer. Figure 2(d) and 2(h) shows the sample prepared with ZnO/SnO_2 bilayer. The visible rough and irregular structure of the thin film implies that the configuration enhances the formation of SnO_2 aggregation.

Figure 3 displays the AFM images of various ETLs deposited on FTO substrates. The corresponding surface roughness values of the samples are shown in Table 1. The AFM results are in good agreement with FESEM results shown earlier. When the SnO_2/ZnO bilayer was deposited on FTO, the surface roughness reduced to 25±1 nm, significantly lower than that of ZnO thin film (36±1 nm). However, when the ZnO/SnO_2 bilayer was deposited on the FTO, it demonstrated the highest surface roughness of 51±3 nm. Figure 3(c) shows that the particles

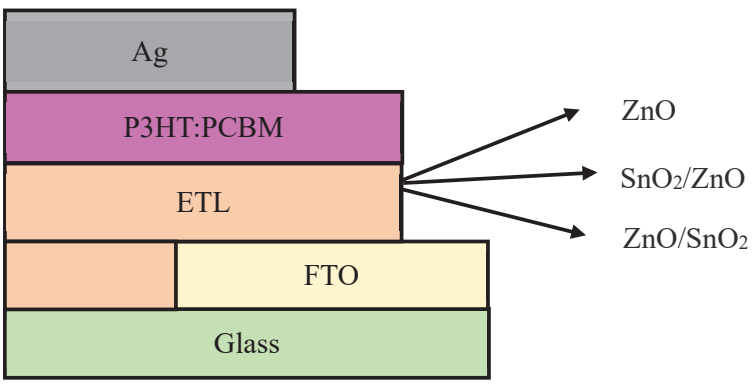

FIGURE 1. Device configuration

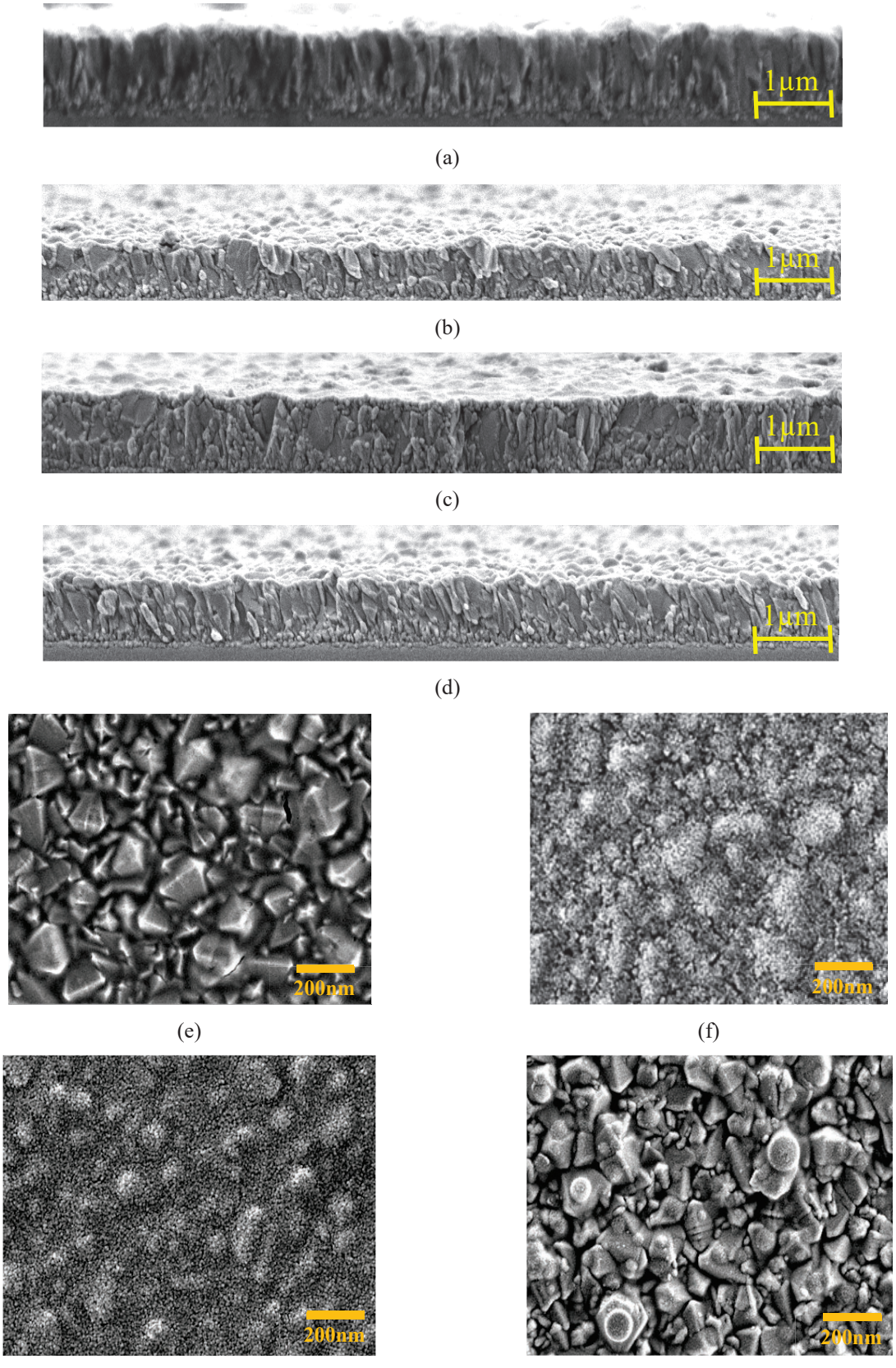

FIGURE 2. Cross sectional FESEM images of (a) SnO_2, (b) ZnO, (c) SnO_2/ZnO, and (d) ZnO/SnO_2 thin films and top surface FESEM images of (e) SnO_2, (f) ZnO, (g) SnO_2/ZnO, and (h) ZnO/SnO_2 thin films

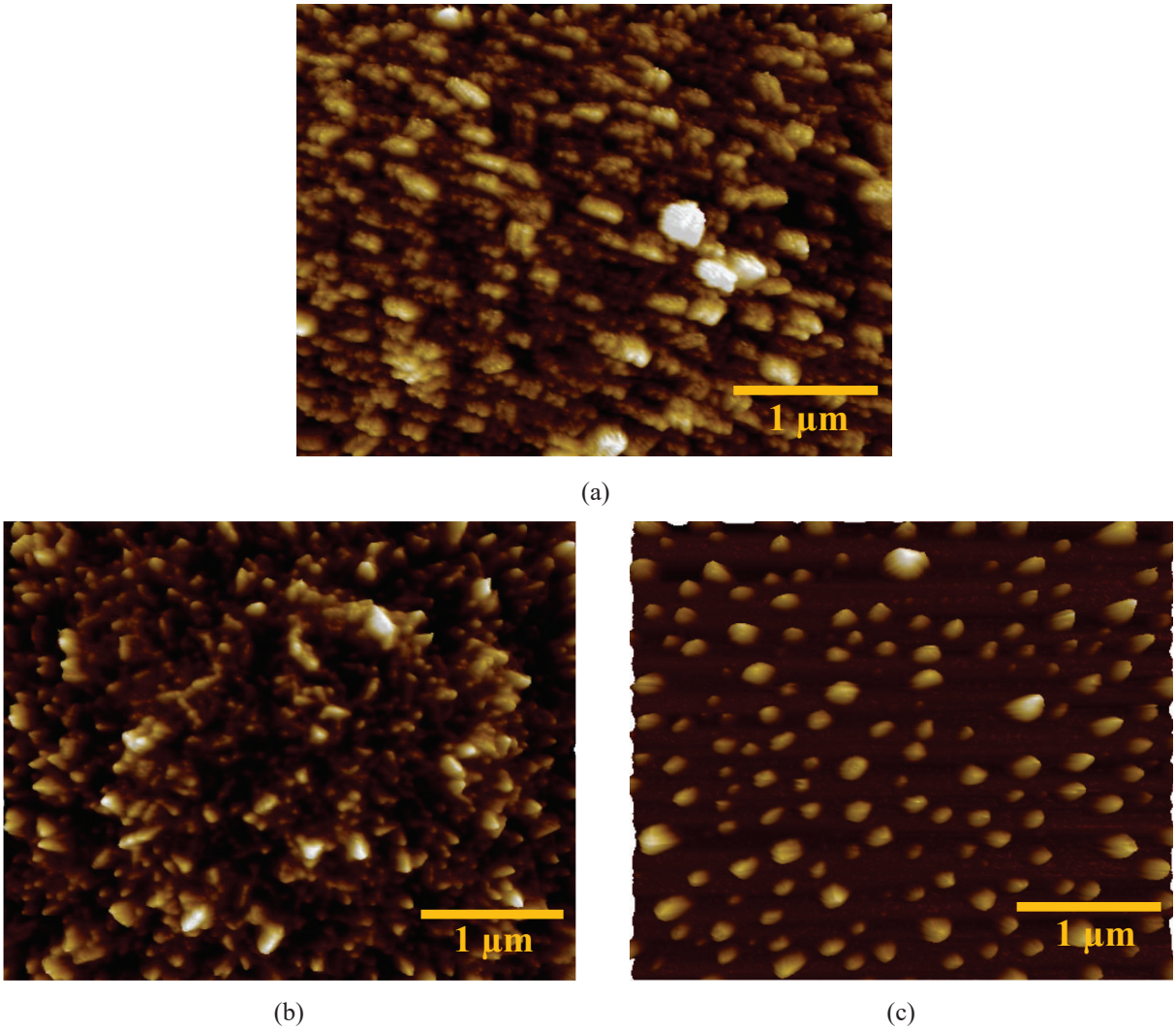

(a)

(b) (c)

FIGURE 3. AFM images of samples with (a) ZnO (b) SnO_2/ZnO and (c) ZnO/SnO_2 thin films

TABLE 1. RMS roughness of thin films

Thin films	RMS roughness, Rq (nm)
FTO/ZnO	36±1
FTO/SnO_2/ZnO	25±1
FTO/ZnO/SnO_2	51±3

on the ZnO/SnO_2 surface are much sharper and farther from one another compared to ZnO thin film (Figure 3(a)). This configuration had increased the aggregation of SnO_2 particles, forming larger structures and leading to higher surface roughness.

The current density-voltage (J-V) characteristics of the devices under 1-sun illumination are shown in Figure 4 and the photovoltaic properties are tabulated in Table 2. The reported photovoltaic parameters are the average values for at least six devices prepared for each variation. Under 1-sun illumination, the control device with only ZnO thin film as ETL obtained a PCE of 0.62 with a V_{oc} of 0.42 V and a J_{sc} of 4.54 mAcm^{-2}. When the devices were prepared with SnO_2/ZnO bilayer ETL, a simultaneous enhancement in the V_{oc}, J_{sc}, FF, and PCE were obtained. This contributes to an increase of 63% in the PCE of the device. However, the devices with ZnO/SnO_2 ETL had shown a decrease in Voc, Jsc as well as PCE with respect to the control device. To get a better understanding of the effects of different configurations of ETLs on the photovoltaic performance, various characterizations were conducted.

One of the requirements of a good ETL includes good light transmittance in the visible range in order to reduce energy loss. Figure 5 shows the optical transmission spectra of various ETLs. The sample with FTO/SnO_2/ZnO configuration demonstrated the highest optical transmittance compared to those of single ZnO as well as ZnO/SnO_2 layers. By adding SnO_2 layer in between FTO and ZnO, the antireflective characteristic of SnO_2 nanoparticles had enabled a greater number of photons to reach the photoactive layer, thus generating more electron-hole pairs (Chandralekha et al. 2024). However, as shown by the AFM characterization, the rough surface of ZnO/SnO_2 layer reduced the light transmission probably due to scattering effect (Harada et al. 2013). The aggregation of SnO_2 might scatter the light and decrease the light from reaching the photoactive layer. The trend of J_{sc} is consistent with the optical transmission, indicating the improvement of J_{sc} is partly due to increased number of photons reaching photoactive layer. Due to the much lower intensity of indoor light, high optical transmission is important to ensure the generation of photocurrent is maximised (Yu et al. 2022a).

PL was carried out to determine the dissociation of excitons in the photoactive layer. The reduction in the recombination of the excitons can be seen through the PL spectra as shown in Figure 6. In addition to the interface between P3HT and PCBM, the excitons can also be dissociated at the P3HT/ETL interfaces. The lowest PL intensity of SnO_2/ZnO ETL samples indicates the most efficient separation of photogenerated charge carriers. In consistence with the FESEM and AFM results, the low surface roughness of SnO_2/ZnO ETL leads to an improved interfacial quality between P3HT and ETL. Due to the rough surface structure of ZnO/SnO_2 ETL, the charge carriers transfer between the photoactive layer and ETL is not efficient compared to the control sample with ZnO ETL, probably due to incomplete coverage and uneven formation of the photoactive layer (Dahal et al. 2022).

Figure 7 shows the energy level diagram of the devices with ZnO and SnO_2/ZnO bilayer ETLs. The work functions of ZnO and SnO_2/ZnO bilayer ETLs were obtained from Kelvin Probe Force Microscopy (KPFM) characterization. KPFM characterization conducted on ZnO/SnO_2 bilayer ETL failed to provide acceptable work function value, which is likely due to poor film formation and large aggregation of SnO_2. A proper energy-level alignment between the conduction band of the ETL and the photoactive layer is crucial to minimize energy loss during charge carrier transfer and facilitate electron extraction. A good energy-level alignment at the interfaces also reduces the energy barrier at the interface to avoid undesirable recombination of electrons and holes. With the addition of the SnO_2 layer, the work function of ETL increased slightly from 4.2 to 4.3 eV. The energy difference between the lowest unoccupied molecular orbital (LUMO) of PCBM and work function of ETL became larger. The larger energy offset creates a driving force that enhances the electron transfer from PCBM to ETL, which then contributes to the enhancement of the electrons extraction as well as allowing electrons to flow smoothly from photoactive layer toward FTO cathode (Davis et al. 2011). In addition to energy level alignment, with a reduced surface roughness, the SnO_2/ZnO ETL also made a good contact with the photoactive layer, resulting in efficient electron extraction and minimized interface recombination. This finding is further supported by the lowest series resistance (R_s) and the highest shunt resistance (R_{sh}) obtained for SnO_2/ZnO ETL device. As a result, the optimum FF, V_{oc}, J_{sc} as well as the PCE have been achieved for SnO_2/ZnO ETL device. As for the ZnO/SnO_2 device, the poor photovoltaic performance could be attributed to the increase in the resistance to the flow of electrons from photoactive layer to the cathode because

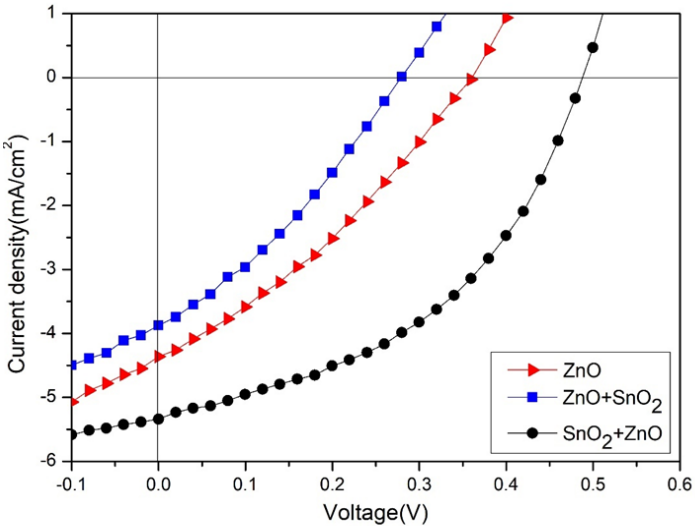

FIGURE 4. J-V characteristics of the devices with different ETLs under AM 1.5G 100 $mWcm^{-2}$ illumination

TABLE 2. Photovoltaic parameters of the devices with different ETLs under AM 1.5G 100 mWcm^{-2} illumination

ETL	V_{oc}[V]	J_{sc}[mAcm^{-2}]	FF[%]	PCE[%]	R_s[Ωcm^2]	R_{sh}[Ωcm^2]
ZnO only	0.42±0.03	4.54±0.27	33±2	0.62±0.02	44	327
SnO_2/ZnO	0.50±0.03	5.51±0.27	37±2	1.01±0.05	35	344
ZnO/ SnO_2	0.34±0.03	3.79±0.34	29±2	0.38±0.04	46	265

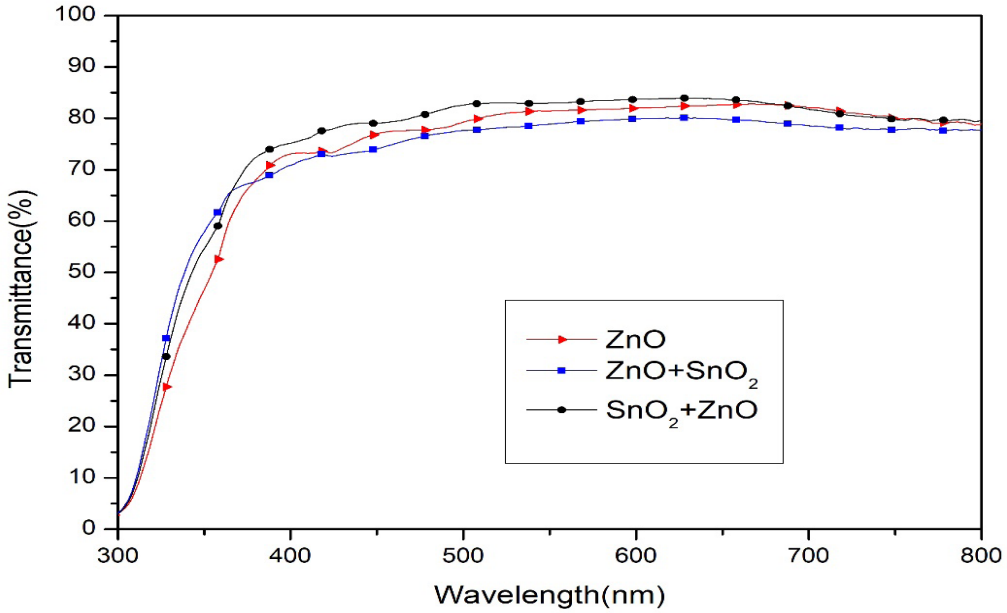

FIGURE 5. Transmission spectra of the samples with various ETLs

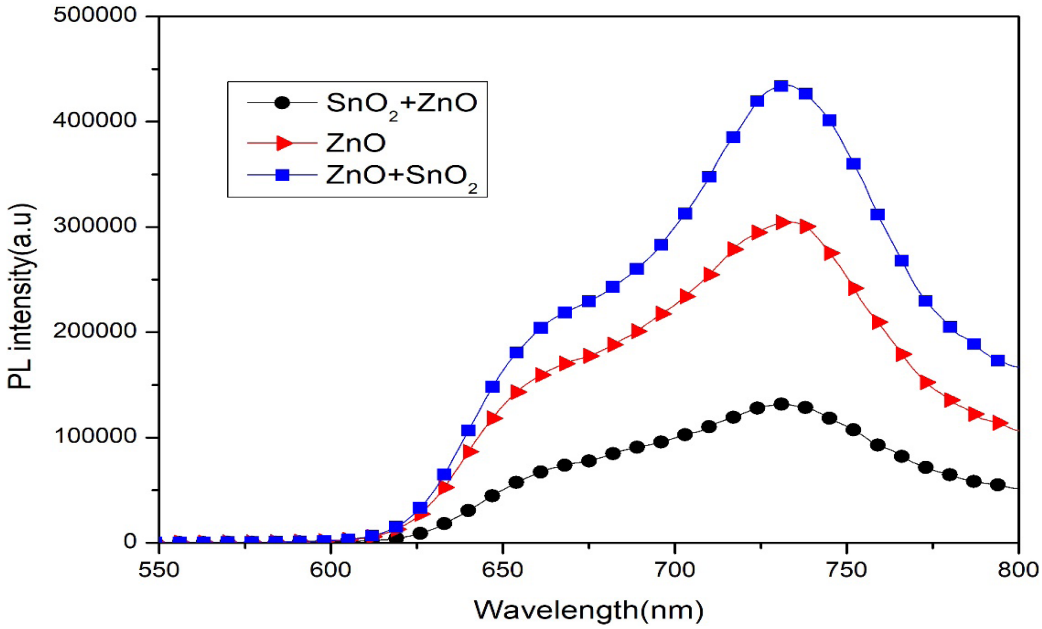

FIGURE 6. Photoluminescence spectra of the samples with various ETLs

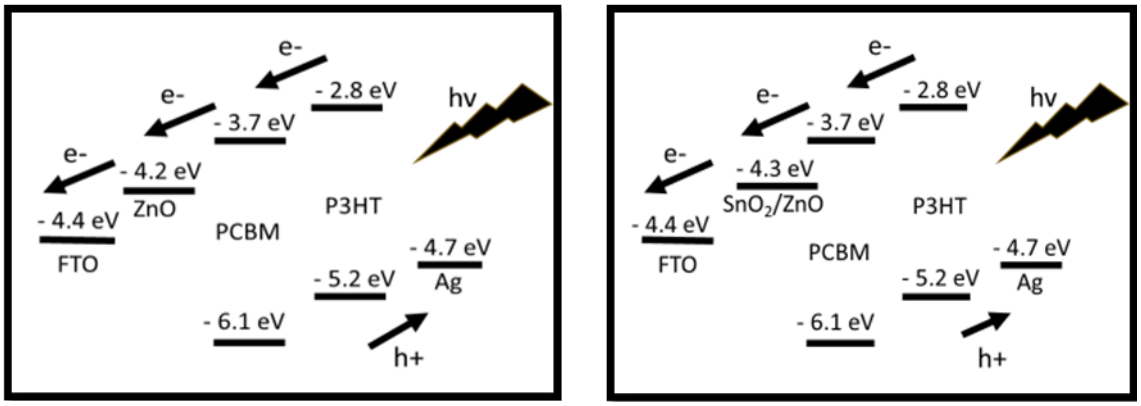

(a) (b)

FIGURE 7. Energy level diagram and work function of (a) ZnO and (b) SnO_2/ZnO ETLs

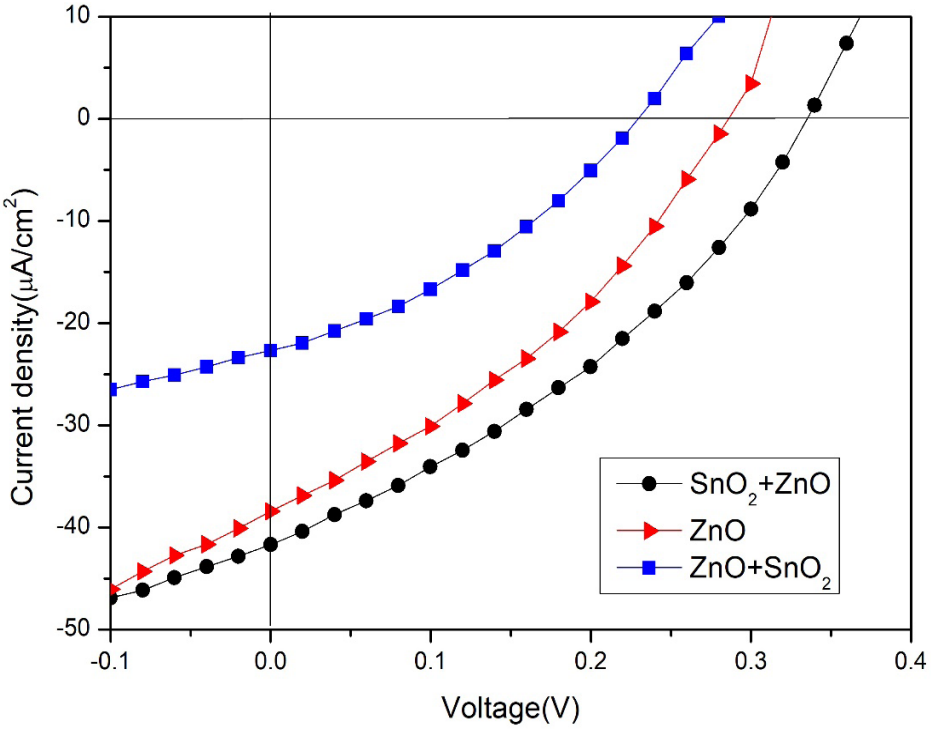

FIGURE 8. J-V characteristics of the devices with different ETLs under white LED illumination

TABLE 3. Photovoltaic parameters of the devices under white LED illumination (1000 lx ≈ 0.28 mWcm^{-2})

Cathode interlayer	V_{oc}[V]	J_{sc}[μAcm^{-2}]	FF[%]	PCE[%]
ZnO only	0.32±0.02	41.2±2.1	26±1	1.25±0.09
SnO_2/ZnO	0.36±0.02	44.8±2.2	28±2	1.62±0.13
ZnO/SnO_2	0.26±0.02	27.1±1.9	21±1	0.54±0.08

of the rough and irregular structure of the ZnO/SnO_2. This then reduced the collection of electrons at the cathode due to the recombination of the photogenerated charge carriers at the interface.

The J-V characteristics of the devices under white LED illumination are shown in Figure 8 and the photovoltaic properties are summarized in Table 3. There is a significant improvement in the PCEs of the samples under white LED illumination compared to those under 1-sun illumination. This is due to a better spectral match between white LED spectrum and the absorbance of the photoactive layer (Wajidh et al. 2023). A similar behaviour of photovoltaic performance was observed under the illumination of solar simulator and white LED. The SnO_2/ZnO ETL device demonstrated the highest V_{oc} of 0.36 V and J_{sc} of 44.8 μAcm^{-2}. Since low-powered electronic devices consume electric power in the range of 1 to 100 μW under idle or standby state (Alkhalayfeh et al. 2022; Khairulaman, Yap & Hj Jumali 2021), based on the P_{max} obtained from the devices, it can be concluded that the devices fabricated in this work are suitable for indoor applications.

CONCLUSION

This study provides an efficient approach to enhance the performance of P3HT:PCBM-based inverted OSCs through modification of the ETL. A bilayer ETL composed of SnO_2 layer at the bottom and ZnO thin film at the top improved the photovoltaic parameters by enhancing the optical transmission, decreasing the surface roughness and providing a well-matched energy level. It is interesting to find that under both 1-sun and white LED illumination, the devices with SnO_2/ZnO ETL demonstrated the highest PCE of 1.01% and 1.62%, an enhancement of 63% and 30% with respect to the control device that consisted of ZnO only ETL.

ACKNOWLEDGEMENTS

The research was funded by Universiti Kebangsaan Malaysia through Research University Grant (GUP) under the grant number (GUP-2024-044). The analytical services were provided by i-CRIM Centralized Lab, Universiti Kebangsaan Malaysia.

REFERENCES

Alkhalayfeh, M.A., Abdul Aziz, A., Pakhuruddin, M.Z., Katubi, K.M.M. & Ahmadi, N. 2022. Recent development of indoor organic photovoltaics. *Physica Status Solidi (a)* 219(5): 2100639. https://doi.org/10.1002/PSSA.202100639

Chandralekha, N.R., Shanthi, J., Swathi, R. & Anoop, K.K. 2024. Enhanced optical performance of solar cell using hydrophobic SnO_2/TEOS/MTMS antireflection coating. *Environmental Progress & Sustainable Energy* 43(5): e14436. https://doi.org/10.1002/ep.14436

Dahal, B., Guo, R., Pathak, R., Rezaee, M.D., Elam, J.W., Mane, A.U. & Li, W. 2022. Enhancing the performance of the perovskite solar cells by modifying the SnO_2 electron transport layer. *Journal of Physics and Chemistry of Solids* 181: 111532. https://doi.org/10.1016/j.jpcs.2023.111532

Davis, R.J., Lloyd, M.T., Ferreira, S.R., Bruzek, M.J., Watkins, S.E., Lindell, L., Sehati, P., Fahlman, M., Anthony, J.E. & Hsu, J.W.P. 2011. Determination of energy level alignment at interfaces of hybrid and organic solar cells under ambient environment. *J. Mater. Chem.* 21(6): 1721-1729. https://doi.org/10.1039/C0JM02349C

Gao, H., Wei, X., Yu, R., Cao, F.Y., Gong, Y., Ma, Z., Cheng, Y.J., Hsu, C.S. & Tan, Z. 2022. Coordination-induced defects elimination of SnO_2 nanoparticles via a small electrolyte molecule for high-performance inverted organic solar cells. *Advanced Optical Materials* 10(6): 2102031. https://doi.org/10.1002/ADOM.202102031

Günther, M., Lotfi, S., Rivas, S.S., Blätte, D., Hofmann, J.P., Bein, T. & Ameri, T. 2023. The neglected influence of zinc oxide light-soaking on stability measurements of inverted organic solar cells. *Advanced Functional Materials* 33(13): 2209768. https://doi.org/10.1002/ADFM.202209768

Harada, T., Murotani, H., Matumoto, S. & Honda, H. 2013. Influence of substrate surface roughness on light scattering of TiO_2 optical thin films. *Chinese Optics Letters* 11(S1): S10303. https://doi.org/10.3788/col201311.s10303

Jiang, Y., Sun, L., Jiang, F., Xie, C., Hu, L., Dong, X., Qin, F., Liu, T., Hu, L., Jiang, X. & Zhou, Y. 2019. Photocatalytic effect of ZnO on the stability of nonfullerene acceptors and its mitigation by SnO_2 for nonfullerene organic solar cells. *Materials Horizons* 6(7): 1438-1443. https://doi.org/10.1039/C9MH00379G

Khairulaman, F.L., Yap, C.C. & Hj Jumali, M.H. 2021. Improved performance of inverted type organic solar cell using copper iodide-doped P3HT:PCBM as active layer for low light application. *Materials Letters* 283: 128827. https://doi.org/10.1016/J.MATLET.2020.128827

Li, H., Yu, B. & Yu, H. 2024. An efficient and stable inverted structure organic solar cell using ZnO modified by 2D $ZrSe_2$ as a composite electron transport layer. *Advanced Functional Materials* 34(37): 2402128. https://doi.org/10.1002/ADFM.202402128

Mahajan, P., Ahmed, A., Datt, R., Gupta, V. & Arya, S. 2022. Chemically synthesized ZnO-WO 3 nanoparticles as electron and hole transport layer in organic solar cells. *ECS Transactions* 107(1): 9199-9209. https://doi.org/10.1149/10701.9199ECST

Mohamed Nafeer Wajidh, Nour Attallah Issa, Kam Sheng Lau, Sin Tee Tan, Chin-Hua Chia, Muslizainun Mustapha, Mohammad Hafizuddin bin Jumali & Chi Chin Yap. 2024. Enhancing indoor photovoltaic performance of inverted type organic solar cell by controlling photoactive layer solution concentration. *Sains Malaysiana* 53(10): 3511-3520. http://doi.org/10.17576/jsm-2024-5310-23

Mussabekova, A.K., Ilyassov, B.R., Aimukhanov, A.K., Tussupbekova, A.K., Zeinidenov, A.K., Valiev, D., Paygin, V., Kudryashov, V.V. & Zhakanova, A.M. 2023. Promising SnOx electron transport layer for polymer solar cells. *Physica B: Condensed Matter* 666: 415113. https://doi.org/10.1016/J.PHYSB.2023.415113

Nam, M., Huh, J.Y., Park, Y., Hong, Y.C. & Ko, D.H. 2018. Interfacial modification using hydrogenated TiO_2 electron-selective layers for high-efficiency and light-soaking-free organic solar cells. *Advanced Energy Materials* 8(14): 1703064. https://doi.org/10.1002/AENM.201703064

Nurul Nadhirah binti Md Ridzuan & Chi Chin Yap. 2022. Kesan suhu rendaman dan suhu sepuh lindap dalam penyediaan filem nipis bismut sulfida (Bi_2S_3) terhadap prestasi sel suria organik jenis songsang berasaskan P3HT: PCBM. *Sains Malaysiana* 51(12): 4099-4110. http://doi.org/10.17576/jsm-2022-5112-18

Omarbekova, G.I., Ilyassov, B.R., Aimukhanov, A.K., Valiev, D.T., Zeinidenov, A.K. & Kudryashov, V.V. 2022. The role of surface defects in the charge transport in organic solar cells based on oxidized indium thin films. *Surfaces and Interfaces* 31: 102026. https://doi.org/10.1016/J.SURFIN.2022.102026

Sabri, N.S., Yap, C.C., Yahaya, M., Mat Salleh, M. & Hj Jumali, M.H. 2017. Solution-dispersed CuO nanoparticles as anode buffer layer in inverted type hybrid organic solar cells. *Physica Status Solidi (A) Applications and Materials Science* 214(1): 1600418. https://doi.org/10.1002/PSSA.201600418

Shim, J.W., Zhou, Y., Fuentes-Hernandez, C., Dindar, A., Guan, Z., Cheun, H., Kahn, A. & Kippelen, B. 2012. Studies of the optimization of recombination layers for inverted tandem polymer solar cells. *Solar Energy Materials and Solar Cells* 107: 51-55. https://doi.org/10.1016/J.SOLMAT.2012.08.004

Suo, Z., Xiao, Z., Li, S., Liu, J., Xin, Y., Meng, L., Liang, H., Kan, B., Yao, Z., Li, C., Wan, X. & Chen, Y. 2023. Efficient and stable inverted structure organic solar cells utilizing surface-modified SnO_2 as the electron transport layer. *Nano Energy* 118: 109032. https://doi.org/10.1016/J.NANOEN.2023.109032

Tarique, W.B., Rahaman, M.H., Dipta, S.S., Howlader, A.H. & Uddin, A. 2024. Solution-processed bilayered ZnO electron transport layer for efficient inverted non-fullerene organic solar cells. *Nanomanufacturing* 4(2): 81-98. https://doi.org/10.3390/NANOMANUFACTURING4020006

Wajidh, M.N., Yap, C.C., Issa, N.A., Lau, K.S., Tan, S.T., Hj Jumali, M.H., Mustapha, M. & Chia, C.H. 2023. Photovoltaic performance improvement of inverted type organic solar cell by co-introducing isopropanol and carbon quantum dots in photoactive layer. *Journal of Materials Science: Materials in Electronics* 34(13): 1075. https://doi.org/10.1007/S10854-023-10489-5

Wang, Y. & Tan, S.T. 2022. Composition of electron transport layers in organic solar cells (OSCs). *Highlights in Science, Engineering and Technology* 12: 99-105. https://doi.org/10.54097/HSET.V12I.1411

Yang, S. & Yu, H. 2023. The modification of ZnO surface with natural antioxidants to fabricate highly efficient and stable inverted organic solar cells. *Chemical Engineering Journal* 452: 139658. https://doi.org/10.1016/J.CEJ.2022.139658

Yang, W., Luo, Z., Sun, R., Guo, J., Wang, T., Wu, Y., Wang, W., Guo, J., Wu, Q., Shi, M., Li, H., Yang, C. & Min, J. 2020. Simultaneous enhanced efficiency and thermal stability in organic solar cells from a polymer acceptor additive. *Nature Communications* 11: 1218. https://doi.org/10.1038/s41467-020-14926-5

Yao, J., Qiu, B., Zhang, Z.G., Xue, L., Wang, R., Zhang, C., Chen, S., Zhou, Q., Sun, C., Yang, C., Xiao, M., Meng, L. & Li, Y. 2020. Cathode engineering with perylene-diimide interlayer enabling over 17% efficiency single-junction organic solar cells. *Nature Communications* 11: 2726. https://doi.org/10.1038/S41467-020-16509-W

Yu, R., Shi, R., Liu, H., Wu, G., Ma, Z., Gao, H., He, Z. & Tan, Z. 2022a. Self-assembly metal chelate as ultraviolet filterable interface layer for efficient organic solar cells. *Advanced Energy Materials* 12(31): 2201306. https://doi.org/10.1002/AENM.202201306

Yu, R., Wei, X., Wu, G., Zhang, T., Gong, Y., Zhao, B., Hou, J., Yang, C. & Tan, Z. 2022b. Efficient interface modification via multi-site coordination for improved efficiency and stability in organic solar cells. *Energy and Environmental Science* 15(2): 822-829. https://doi.org/10.1039/D1EE03263A

Zhou, Y., Fuentes-Hernandez, C., Shim, J., Meyer, J., Giordano, A.J., Li, H., Winget, P., Papadopoulos, T., Cheun, H., Kim, J., Fenoll, M., Dindar, A., Haske, W., Najafabadi, E., Khan, T.M., Sojoudi, H., Barlow, S., Graham, S., Brédas, J-L., Marder, S.R., Kahn, A. & Kippelen, B. 2012. A universal method to produce low–work function electrodes for organic electronics. *Science* 336(6079): 327-332. https://doi.org/10.1126/science.1218829

*Corresponding author; email: ccyap@ukm.edu.my